

Impact of copper nanoparticles and copper ions on transcripts involved in neural repair mechanisms in rainbow trout olfactory mucosa

parastoo Razmara (✉ razmara@ualberta.ca)

University of Alberta <https://orcid.org/0000-0003-3286-0825>

Gregory Pyle

University of Lethbridge

Research Article

Keywords: Copper nanoparticles, olfactory mucosa, neuroregeneration, axon 43 regeneration, rainbow trout.

Posted Date: July 14th, 2022

DOI: <https://doi.org/10.21203/rs.3.rs-1805285/v1>

License:   This work is licensed under a Creative Commons Attribution 4.0 International License.

[Read Full License](#)

1 **Impact of copper nanoparticles and copper ions on transcripts involved in neural repair**
2 **mechanisms in rainbow trout olfactory mucosa**

3 Parastoo Razmara*, Gregory G. Pyle

4 Department of Biological Sciences, University of Lethbridge, Lethbridge, Alberta, Canada.

5

6 *Corresponding author: Parastoo Razmara. Present address: Department of Biological Sciences,
7 Z-620 Biological Sciences Bldg., University of Alberta, Edmonton, Alberta, Canada, T6G 2E9.

8 Email: razmara@ualberta.ca

9

10 **Running head:** Effect of nanocopper on repair pathway in olfactory mucosa

11

12

13

14

15

16

17

18

19

20

21 **Abstract**

22 Olfactory mucosa is well-known for its lifelong ability for regeneration. Regeneration of
23 neurons and regrowth of severed axons are the most common neural repair mechanisms in
24 olfactory mucosa. Nonetheless, exposure to neurotoxic contaminants, such as copper nanoparticles
25 (CuNPs) and copper ions (Cu^{2+}), may alter the reparative capacity of olfactory mucosa. Here, using
26 RNA-sequencing, we investigated the molecular basis of neural repair mechanisms that were
27 affected by CuNPs and Cu^{2+} in rainbow trout olfactory mucosa. The transcript profile of olfactory
28 mucosa suggested that regeneration of neurons was inhibited by CuNPs. Exposure to CuNPs
29 reduced the transcript abundances of pro-inflammatory proteins which are required to initiate
30 neuroregeneration. Moreover, the transcript of genes encoding regeneration promoters, including
31 canonical Wnt/ β -catenin signaling proteins and developmental transcription factors, were
32 downregulated in the CuNP-treated fish. The mRNA levels of genes regulating axonal regrowth,
33 including the growth-promoting signals secreted from olfactory ensheathing cells, were mainly
34 increased in the CuNP treatment. However, the reduced transcript abundances of a few cell
35 adhesion molecules and neural polarity genes may restrict axonogenesis in the CuNP-exposed
36 olfactory mucosa. In the Cu^{2+} -treated olfactory mucosa, both neural repair strategies were initiated
37 at the transcript level. The stimulation of repair mechanisms can lead to the recovery of Cu^{2+} -
38 induced olfactory dysfunction. These results indicated CuNPs and Cu^{2+} were differentially
39 affected the neural repair mechanism in olfactory mucosa. Exposure to CuNP had greater effects
40 on olfactory repair mechanisms relative to Cu^{2+} and dysregulated the transcripts associated with
41 stem cell proliferation and neural reconstitution.

42 **Keywords:** Copper nanoparticles, olfactory mucosa, neuroregeneration, axon
43 regeneration, rainbow trout.

44 **Introduction**

45 Perception of chemosensory signals conveys information to fish that is essential for
46 survival and reproduction success. Detecting the presence of an appropriate mate, the location of
47 food, the risk of predation, and the presence of potentially toxic contaminants in fish habitat is
48 mediated through olfactory sensory neurons (OSNs). These OSNs receive sensory inputs and
49 transmit them to brain for processing (Kermen et al., 2013; Laberge and Hara, 2001). Due to direct
50 contact of OSNs with myriad biotic and abiotic environmental stressors, they are susceptible to
51 functional impairment. Vertebrate olfactory neuroepithelium is capable of regeneration in response
52 to damage. Reconstitution of damaged OSNs is a key process to restore olfactory function.
53 Nevertheless, some anthropogenic contaminants can interfere with olfactory neuroepithelial
54 regenerative capability, and consequently inhibit the neuroepithelium reestablishment
55 (Szymkowicz et al., 2019; Wang et al., 2017a).

56 Copper nanoparticles (CuNPs) are emerging environmental contaminants of concern
57 (Malhotra et al., 2020). Due to unique conductivity, catalytic, and antimicrobial properties of
58 engineered CuNPs, they appear as a promising material to be applied in electronics, biomedical,
59 and agriculture (Tabesh et al., 2018; Vanti et al., 2020; Zhou et al., 2019). The application of
60 CuNPs as an antibiofouling agent in fish-cage netting (Ashraf et al., 2017), an antibiofilm agent
61 against fish pathogens (Chari et al., 2017), and a dietary supplement to boost fish growth and
62 immune system (El Basuini et al., 2017), make them popular in the aquaculture industry. The
63 progressive production and utilization of CuNPs enhances their incidental input to water bodies.
64 We have previously demonstrated that CuNPs can be taken up by rainbow trout olfactory mucosal
65 cells and induce olfactory toxicity (Razmara et al., 2021). Exposure to CuNPs can not only disrupt
66 OSN function (Razmara et al., 2021; Razmara et al., 2019), but also reduce the transcription of

67 neuroregeneration-related pathways in rainbow trout olfactory mucosa (Razmara et al., 2021). The
68 CuNP-induced olfactory impairment was persisted after 7 days of transition to clean water, and
69 the OSNs function did not restore (Razmara and Pyle, 2022). We also compared the toxicity of
70 CuNP and copper ion (Cu^{2+}) which is a well-known olfactory disrupter. In Cu^{2+} -treated fish, unlike
71 those in the CuNP treatment, neuroregenerative pathways was upregulated (Razmara et al., 2021),
72 and the olfactory function was recovered (Razmara and Pyle, 2022). These findings indicates that
73 CuNPs and Cu^{2+} have differential effects on the neuroregeneration process in the olfactory mucosa.
74 Nonetheless, the detailed regenerative molecular events that were affected by each of the Cu
75 contaminants remain unknown.

76 In addition to OSNs, there are other types of cells residing in the fish olfactory mucosa
77 (Fig. 1). Mucus-secreting goblet cells and sustentacular cells (a.k.a., supporting cells) provide
78 protection and structural functional support to the epithelial cells, respectively (Bols et al., 2001;
79 Hegg et al., 2009). Basal stem cells are involved in regeneration processes of epithelial cells. Two
80 types of neural repair mechanisms have been reported in a damaged olfactory mucosa. First is the
81 genesis of new OSNs from the basal stem cells (Graziadei and Graziadei, 1979). Olfactory neural
82 replenishment is a complex multiphase process that entails progenitors forming from olfactory
83 stem cells followed by migration and differentiation, which ultimately gives rise to mature OSNs
84 (Nicolay et al., 2006). The basal layer of olfactory epithelium is composed of two populations of
85 stem cells, horizontal basal cells (HBCs) and globose basal cells (GBCs) (Fig. 1) (Roy et al., 2013).
86 In general, GBCs are mitotically active, whereas the HBCs are a reserve population which remains
87 mitotically quiescent under conditions of non-extensive injury (Choi and Goldstein, 2018). To
88 maintain the integrity of olfactory neuroepithelium, both classes of stems cells are actively
89 interacting with extrinsic regulators (e.g., immune cells) in their niche (Chen et al., 2019). These

90 intercellular interactions lead to activation of intrinsic regulators, such as transcription factors, that
91 control stem cell proliferation, differentiation, and neuron maturation. The second type of repair is
92 axonal regrowth in existing OSNs. During axon regeneration a specialized type of glial cell,
93 olfactory ensheathing cell (OEC), secretes extrinsic growth and guidance cues and subsequently,
94 reactivates the intrinsic developmental process in the growing axon (Roet and Verhaagen, 2014).
95 In this study, using the transcription profile of rainbow trout olfactory mucosa, we investigated
96 how exposure to CuNPs and Cu²⁺ differentially affected intrinsic and extrinsic regeneration
97 regulators.

98 **Materials and Methods**

99 **Fish husbandry and experimental design**

100 Juvenile rainbow trout with an average weight of 26.5 ± 5.2 g (mean \pm SD; n = 15) were
101 obtained from Sam Livingston Fish Hatchery (Alberta, Canada) and housed in a holding tank (16
102 h light: 8 h dark photoperiod, 12 °C) at the University of Lethbridge Aquatic Research Facility
103 (ARF). According to our previous study, the 50% olfactory inhibitory concentrations of CuNPs
104 and Cu²⁺ (24-h IC₅₀ measured by electro-olfactography) were 320 ± 13 and 7 ± 1 µg/L (mean \pm
105 SD), respectively (Razmara et al., 2019). These IC₅₀s of Cu contaminants were used as a
106 functional unit of toxicity. Following a two-week acclimation period, to investigate the
107 comparative effect of CuNPs and Cu²⁺ on the transcript profiles of rainbow trout olfactory mucosa,
108 fish were exposed to 24-h IC₅₀s of Cu contaminant for 96 h (Razmara et al., 2021). Every 24 h,
109 fish were transferred to new sets of tanks containing fresh water and Cu solutions. Quality of
110 culture water was measured as follows (mean \pm SD; n = 3): temperature, 12.4 ± 0.3 °C; dissolved
111 oxygen, 8.8 ± 0.7 mg/L; conductivity, 331.3 ± 0.3 µS /cm; hardness, 156 ± 3.1 mg/L as CaCO₃;

112 alkalinity: 125.0 ± 4.4 mg/L as CaCO_3 ; median pH, 8.1 (range 7.8 – 8.4), and dissolved organic
113 carbon, 2.5 ± 0.7 mg/L. During the exposure period fish were not fed.

114 **Preparation of Cu stock mixtures, Cu analysis, and CuNPs characterization**

115 Copper solution preparation and analysis were described by Razmara et al., 2021. In short,
116 using a 30 min water bath sonicator (UD 150SH6LQ; 150 W; Eumax; USA), nanocopper powder
117 (35 nm; 99.8% purity; partially passivated, Nanostructured & Amorphous Materials Inc, USA)
118 was suspended in ddH₂O (18.2 MΩ/cm water, Millipore, USA) to make a stock suspension of 250
119 mg/L CuNPs. A fresh stock solution of 100 mg/L CuSO_4 (>98% purity; BHD, USA) in ddH₂O
120 was prepared and used as the source of Cu^{2+} . The actual concentration of Cu in the fish tanks was
121 measured by graphite furnace atomic absorption spectrometry (240FS GFAAS, Agilent
122 Technologies, USA). The actual Cu^{2+} and CuNPs concentrations 24 h after spiking the fish tanks
123 with Cu mixtures, were 7 ± 1 μg/L and 210 ± 13 μg/L (65% of nominal CuNPs concentration),
124 respectively (mean ± SD, n = 6) (Razmara et al., 2021). The Cu concentration in the control was
125 below the GFAAS detection limit.

126 We previously characterized the CuNPs (Razmara et al., 2019), and we used the same batch
127 nanocopper powder for this study. The CuNPs were semi-spherical with an average diameter of
128 32 ± 1 nm (mean ± SEM). Polydispersity index (PDI), hydrodynamic diameter (HDD), and zeta
129 potential, which are indicators of NP aggregation, were changed over 24 h. Sixteen h after spiking
130 the fish tanks water with CuNPs, we observed a significant increase in polydispersity (PDI = 1)
131 and HDD, along with a noticeable reduction in zeta potential. These measurements indicated
132 CuNPs were less stable and consequently, less bioavailable over the last few hours of exposure
133 (Razmara et al., 2019). Using Amicon Ultra-4 Centrifugal Filter Units (3K regenerated cellulose
134 membrane, Merck Millipore Ltd., USA), dissolved Cu was separated from CuNPs. The

135 concentration of dissolved Cu in the filtrate was measured using GFAAS over 24 h (Razmara et
136 al., 2019). We observed a gradual release of dissolved Cu in the fish tanks over time (the highest
137 dissolution after 24 h was 14 µg/L) (Razmara et al., 2019). Therefore, the effects of CuNPs on
138 olfactory mucosa is associated to both nanocopper and dissolved Cu.

139 **RNA isolation**

140 As described in Razmara et al. (2021), following the 96-h exposure to CuNPs and Cu²⁺,
141 fish (n = 5) were euthanized using a pH buffered MS222 solution (240 mg/L tricaine methane
142 sulfonate (AquaLife, Canada) and 720 mg/L NaHCO₃ (Fisher Scientific, USA)). Immediately after
143 euthanizing, fish olfactory rosettes were dissected, flash-frozen in liquid nitrogen, and stored in -
144 80°C. Using RNeasy Mini Kit manufacturer's protocol (catalogue # 74106; Qiagen), total RNA
145 was isolated from olfactory rosettes. Quality and quantity of isolated RNA were determined by a
146 Nanodrop spectrophotometer (Thermo Scientific NanoDrop One spectrophotometer, Thermo
147 Scientific). The RNA integrity number (RIN) was determined by Bioanalyzer 2100 (Agilent
148 Technologies). The RIN of all samples were > 7 (Razmara et al., 2021).

149 **Illumina sequencing and RNA-seq analysis**

150 High quality RNA samples were shipped to Canada's Michael Smith Genome Sciences Centre
151 (GSC, BC cancer research, Canada) to construct strand specific mRNA libraries. Each library was
152 sequenced using the HiSeq 2500 (Illumina, San Diego, California, USA) as paired-end platform
153 generating 2 * 75 base pair (bp) reads for each sample (Razmara et al., 2021). The RNA-seq
154 analysis pipeline is fully described in Razmara et al. (2021). In brief, reads were assessed for their
155 quality using FastQC (Andrews, 2020), and high quality reads were aligned to rainbow trout
156 reference transcriptome (Omyk_1.0, GCF_002163495.1) using STAR two-pass alignment version
157 2.6.1 (Dobin et al., 2013). Using StringTie version 1.3.4, mapped reads were assembled and

158 counted (Pertea et al., 2015). The counted transcripts were annotated against National Center for
159 Biotechnology Information (NCBI) non-redundant (nr) protein database using BLASTx.
160 Differential gene expression analyses was conducted using DESeq2 version 1.28.1 (Love et al.,
161 2014) with a $p_{\text{adj}} \leq 0.05$ cut-off for statistical significance. Of the total number of transcripts in
162 Cu^{2+} (53141) and CuNPs (53380) treatments, 2.1% were differentially expressed in each treatment.
163 However, there was a narrow overlap between the CuNP- and Cu^{2+} - affected transcripts (Razmara
164 et al., 2021). The functional annotations of the differentially expressed transcripts was performed
165 in Blast2Go Pro (OmicsBox version 1.3.11) (Götz et al., 2008). The functional annotation analysis
166 showed 87% and 89% of the differentially expressed transcripts were functionally annotated in
167 CuNPs and Cu^{2+} treatment, respectively (Razmara et al., 2021). Enrichment analysis of gene
168 ontology (GO) terms was conducted using the Fisher's exact test in Blast2GO ($p \leq 0.05$).

169 **Gene expression quantification by qPCR**

170 The results of RNA-seq were previously validated and confirmed by qPCR gene expression
171 (Razmara et al., 2021). In this study, the expression *TCF7L2*, a key transcription factor involved
172 in Wnt signaling pathway, was studied in both Cu treatments using qPCR. One μg of the total
173 RNA was used to make cDNA using (QuantiTec Reverse Transcription Kit, catalogue # 205311,
174 Qiagen). The *TCF7L2* primer set was designed using Primer-Blast online software provided by
175 NCBI (Ye et al., 2012). To ensure the specificity of the primers' amplification, the PCR products
176 were purified (QIAquick PCR Purification kit, catalogue # 28104; Qiagen), sequenced, and blasted
177 in NCBI. The primer sequences for *TCF7L2* (primer efficiency: 102%) were as follows: F -
178 CGAATCAAAGTCCGAACGCA, R - TTTGGAAACGCCGTCGAGA. The quantification of
179 gene expression analysis was carried out in duplicate on a Bio-Rad thermocycler (C1000 Touch
180 thermocycler, CFX96 Real-Time System, Bio-Rad) using RT² SYBR Green qPCR master mix

181 (catalogue # 330503, Qiagen) as described by Razmara et al. (2021). Expression of *TCF7L2* was
182 normalized to the expression of reference genes, *ACTB* (Aegerter et al., 2005) and *EF1a* (Polakof
183 et al., 2010), which did not changed in the transcriptome analysis. Quantification of the *TCF7L2*
184 transcripts was analyzed according the Pfaffl method of relative quantification (Pfaffl, 2001). To
185 determine whether *TCF7L2* was differentially expressed in response to (CuNPs and Cu²⁺, we
186 conducted one-way analysis of variance (ANOVA) with Tukey's post hoc test using R, version
187 3.6 (R Core Team, 2019).

188 **Results and discussion**

189 **Effect CuNPs and Cu²⁺ on the repair mechanism in the olfactory mucosa**

190 Results of pathway enrichment analysis indicated a number of neuroregeneration-related
191 functional GO terms, including neurogenesis, were composed of downregulated genes in the CuNP
192 treatment (Fig. 2A). We previously reported that CuNPs, but not Cu²⁺, were significantly
193 accumulated in the olfactory mucosal cells (Razmara et al., 2021). In the CuNP-treated fish, there
194 was a progressive impairment in the olfactory responses over time (Razmara et al., 2019). In
195 consequent of the dysregulated repair mechanisms, the neurophysiological responses of CuNP-
196 exposed OSNs remained impaired after the 7 days of recovery period (Razmara and Pyle, 2022).
197 These results indicate CuNPs had adverse effects on the OSNs which may not be simple to repair.
198 Our current knowledge of possible effects of CuNPs on olfactory neuroregeneration is scarce. In
199 the central nervous system of zebrafish embryos, exposure to copper oxide nanoparticles resulted
200 in reduced neural development (Xu et al., 2017).

201 On the other hand, the upregulation of genes encoding developmental-related pathways in
202 the Cu²⁺ treatment, such as cell cycle and epithelium development (Fig. 2B), reflects that
203 regeneration processes were activated in the olfactory mucosa. Despite a continuous exposure to

204 Cu^{2+} , we previously observed a partial recovery in Cu^{2+} -exposed OSNs function (Razmara et al.,
205 2019). After 7 days of exposure to Cu^{2+} the fish olfactory function was fully recovered (Razmara
206 and Pyle, 2022). This functional olfactory recovery was a further indication of active repair
207 mechanisms in the Cu^{2+} treatment. A 24-h exposure of the olfactory system to Cu^{2+} increased the
208 level of neurogenesis-related miRNAs and mRNAs in zebrafish (Tilton et al., 2008; Wang et al.,
209 2013). Consistent with our results, developmental pathways were enriched in the Cu^{2+} -exposed
210 zebrafish olfactory system (Tilton et al., 2008). A recent study indicated that different classes of
211 OSNs (i.e. ciliated and microvillous OSNs) in zebrafish larvae display distinct reparative responses
212 following a 24-h exposure to 16 – 635 $\mu\text{g/L}$ Cu^{2+} (Ma et al., 2018). Regeneration of microvillous
213 cells occurred following a 72-h recovery period whereas, there was no significant regeneration of
214 ciliated OSNs in the Cu^{2+} -exposed larvae. Nonetheless, ciliated cells showed a partial functional
215 improvement following the recovery period (Ma et al., 2018). These results suggested that in the
216 ciliated OSNs, rather than replacement of the injured OSNs with new neurons, axonal regeneration
217 was activated to repair the Cu^{2+} -induced injuries. Confocal images of Cu^{2+} -exposed zebrafish
218 demonstrated that ciliated OSNs had more axon retractions than microvillous cells (Ma et al.,
219 2018). Axonal retractions can stimulate axonal repair mechanisms in ciliated cells. In our study,
220 the upregulation of genes involved in the cell projection GO term suggests axonogenesis may be
221 activated in both CuNP and Cu^{2+} treatment (Fig. 2).

222 **Inflammatory responses in the CuNP- and Cu^{2+} -exposed olfactory mucosa**

223 In addition to the defensive role of inflammatory response pathway in the olfactory
224 neuroepithelium, inflammation contributed towards the regulation of regeneration (Chang and
225 Glezer, 2018; Chen et al., 2017, 2019; Crisafulli et al., 2018). The results of pathway enrichment
226 analysis showed that genes encoding for proinflammatory chemokines and cytokine signaling were

227 significantly downregulated in the CuNP-treated olfactory mucosa (Fig. 2A). The reduced
228 transcript abundances of many pro-inflammatory genes including *IL-1 β* , *CCL4*, *CCL19*, *CCL20*,
229 and *CCL25* (Table 1), in the CuNP treatment suggest CuNPs may act as an anti-inflammatory
230 treatment in the rainbow trout olfactory mucosa. Previous studies demonstrated a number of metal
231 NPs, including CuNPs, can have anti-inflammatory properties (Agarwal et al., 2019;
232 Thiruvengadam et al., 2019). Blocking of cytokine signaling is reported as the primary mechanism
233 of anti-inflammation induced by metal NPs (Agarwal et al., 2019).

234 Acute inflammation plays a positive role in neural stem cells function. In the adult zebrafish
235 brain, acute inflammation is required to activate neuroregeneration, and administration of anti-
236 inflammatory dexamethasone (Dex) impeded the regeneration of lesioned brain (Kyritsis et al.,
237 2012). In the mouse olfactory mucosa, repair of lesioned neuroepithelium was also reliant on the
238 induction of acute inflammation (Chen et al., 2017). In Dex-treated mice with low transcript
239 abundances of proinflammatory cytokines, the proliferation and subsequent differentiation of
240 HBCs were significantly impaired (Chen et al., 2017). Moreover, a three-day treatment of lesioned
241 olfactory mucosa with Dex resulted in a marked reduction in the number of regenerated OSNs in
242 mice (Crisafulli et al., 2018). The potential anti-inflammatory properties of CuNP may block stem
243 cell proliferation and neuroregeneration in the olfactory neuroepithelium which needs further
244 investigation.

245 In addition to the low transcript level of *IL-1 β* cytokine in the CuNP treatment, activation
246 of its protein may be impaired by CuNPs. The pro *IL-1 β* needs to be activated by a protein complex
247 known as inflammasome (Liu et al., 2017). The transcript abundances of key components of
248 inflammasomes, including *CASP1*, *NLRP3*, and *MEFV* (encoding pyrin) — which are necessary
249 to cleave the pro *IL-1 β* (Liu et al., 2017; Sharma et al., 2019) — was reduced (Table 1). Previous

250 studies have demonstrated that transient inflammation mediated by IL-1 β promotes regeneration
251 in zebrafish (Hasegawa et al., 2017; Tsarouchas et al., 2018). Inhibiting pro IL-1 β activation by
252 blocking CASP1 activity resulted in weak axonal regeneration in zebrafish spinal cord (Tsarouchas
253 et al., 2018). Moreover, IL-1 β has been reported to promote the olfactory stem cells migration in
254 a concentration-dependent manner in rat neuroepithelium (Pu et al., 2018). Hence, the
255 downregulation of *IL-1 β* and its activators by CuNPs may inhibit olfactory neuroregeneration.

256 One of the primary cellular inflammatory pathways is nuclear factor- κ B (NF- κ B)
257 signaling, which regulates expression of a large array of genes implicated in inflammation
258 including *IL-1 β* and *NLRP3*. The NF- κ B transcription factors mediate two signaling pathways,
259 non-canonical (a.k.a., NIK/NF- κ B signaling) and canonical pathways, which both regulate
260 cellular inflammation despite applying different signalling mechanisms (Liu et al., 2017). The NF-
261 κ B transcription factor family composed of five members, including NF- κ B1 (P50), NF- κ B2
262 (P52), RELA(P65), RELB, and c-REL which are operating as dimeric complexes activating κ B
263 enhancer (Pasparakis, 2009). Pathway enrichment analysis showed the NIK/NF- κ B signaling was
264 over-represented in the CuNP treatment (Fig. 2). In the NIK/NF- κ B signaling pathway,
265 association of specific ligands with tumor necrosis factor superfamily (TNFR), such as CD40,
266 stimulates the production of mature P52 from its precursor p100 (Sun, 2011). Processing of p100
267 is mediated by NF- κ B-inducing kinase (NIK) which activates an inhibitor of NF- κ B kinase (IKK)
268 to subsequently induce phosphorylation and ubiquitination of p100 and generate mature p52 (Sun,
269 2017). The mature p52 forms a heterodimer complex with RELB and, together, translocate to the
270 nucleus to induce the transcription of target genes, such as *CCL19* (Valiño-Rivas et al., 2016).
271 Figure 3A displays that exposure to CuNPs reduced the transcript abundances of *CD40*, *P52* in the
272 NIK/NF- κ B signaling pathway. The canonical NF- κ B pathway was also affected by CuNPs (Fig.

273 3B). In the canonical NF- κ B signaling, different stimuli including cytokines and growth factors
274 activate the IKK to phosphorylate the inhibitor of NF- κ B (I κ B α) and trigger its degradation. The
275 degradation of I κ B α results in nuclear translocation of NF- κ B transcription factor dimers
276 (P50/RELA or P50/c-REL) and initiation of target gene transcriptions (e.g., *IL-1 β* , *NLRP3*, *CCL4*,
277 *CCL20*). In the CuNP-treated olfactory mucosa, while the mRNA level of *c-REL* was reduced, the
278 expression of *I κ B α* was slightly increased (Table 1 and Fig. 3B). The NF- κ B signaling pathway
279 plays a critical role in early stages of neurogenesis. Differentiation of neural stem cells is reliant
280 on the activation of NF- κ B signaling, and inhibition of canonical NF- κ B signaling can block
281 asymmetric cell division which is essential for proper neurogenesis (Zhang et al., 2012). Moreover,
282 impairment of the canonical NF- κ B pathway through deletion of RelA inhibited the
283 neuroregeneration in HBCs (Chen et al., 2017). Impairment of NF- κ B signaling pathway may
284 comprise the acute inflammatory responses in the CuNP-treated olfactory mucosa. Given the
285 importance of acute inflammation in neurogenesis initiation, the downregulation of transcripts
286 associated with canonical and non-canonical NF- κ B inflammatory pathways suggests
287 neuroregeneration was inhibited in the CuNP treatment. This notion is supported by the continued
288 olfactory impairment of CuNP-exposed fish after the 7-day recovery period.

289 In contrast to the CuNP treatment, gene expression of pro-inflammatory cytokines and
290 chemokines remained unchanged in the Cu²⁺ treatment. The expression of *NLRP1b*, an important
291 component of inflammasomes involved in CASP1 activation (de Rivero Vaccari et al., 2014),
292 displayed a significant upregulation in Cu²⁺-treated fish (Table 1). The activation of CASP1 can
293 consequently enhance the pro IL-1 β cleavage and induce inflammation. Furthermore, the transcript
294 abundances of *NLR12* and *NLRC3*, that both negatively regulate the NF- κ B inflammatory
295 signaling (Gharagozloo et al., 2015; Tuncer et al., 2014), were reduced (Table 1). These data

296 suggest that olfactory mucosal cells' inflammatory responses were not inhibited as a result of
297 exposure to Cu^{2+} , and consequently, neurogenesis pathways may be activated.

298 **Effect of Cu contaminants on canonical Wnt/ β -catenin signaling pathway**

299 In addition to the suppression of inflammatory signaling, Wnt signaling, one of the major
300 pathways regulating stem cell proliferation and differentiation, was affected by CuNPs (Fig. 2). In
301 agreement with our results, a transcript-based study on the lungs of mice exposed to inhalation of
302 copper oxide nanoparticles for two weeks, indicated that the Wnt signaling pathway was
303 significantly enriched (Rossner et al., 2020). Furthermore, copper oxide nanoparticles inhibited
304 the Wnt signaling pathway in prostate cancer cells and attenuated the stemness of cancer cells
305 (Wang et al., 2017b).

306 Activation of canonical Wnt/ β -catenin pathway promotes neurogenesis in the olfactory
307 epithelium (Wang et al., 2011). In GBCs, Wnt/ β -catenin pathway plays a key role in maintaining
308 proliferation and promoting neuroregeneration (Chen et al., 2014). Moreover, the activation of
309 Wnt/ β -catenin signaling was both necessary and sufficient to switch the HBCs from a resting state
310 to an activated neurogenic state (Fletcher et al., 2017). In the Wnt/ β -catenin pathway, when the
311 Wnt ligand is present, β -catenin relocates from cytoplasm to the nucleus, where it binds to the
312 TCF/LEF transcription factor to promote the expression of many genes involved in cell
313 proliferation (Bengoa-Vergniory and Kypta, 2015). Inhibition of the Wnt/ β -catenin signaling
314 through disruption of β -catenin/TCF complex transcriptional activity prevented the regeneration
315 of injured olfactory epithelium (Wang et al., 2011). Following exposure to CuNPs, there was a
316 considerable reduction in the expression of *TCF7L2*, which is a downstream effector of the Wnt
317 pathway (Table 1 and Fig. 4A). The *TCF7L2* gene expression analysis by qPCR confirmed the
318 result of RNA-seq (Fig. 4B). Of the 4 members of the TCF/LEF transcription factor family,

319 TCF7L2 was the most expressed transcription factor in the mouse's entire olfactory epithelium,
320 which had a dense expression in basal stem cells (Wang et al., 2011). In zebrafish, TCF7L2
321 positively regulated the Wnt/ β -catenin pathway in midbrain, and TCF/LEF transcription factors
322 contributed in the homeostasis of olfactory epithelium (Shimizu et al., 2012). As a result of the
323 *TCF7L2* downregulation, the neuroregeneration might be reduced in the CuNP-treated fish.

324 In the absence of Wnt, β -catenin is actively degraded by a destruction complex in the
325 cytoplasm, which consequently diminishes the expression of target genes. One of the components
326 of the β -catenin destruction complex is APC (a tumor suppression factor) (Fig. 4A). The APC is a
327 multifunctional protein that not only mediates stem cell maintenance through the regulation of
328 cytoplasm β -catenin, but also promotes neuronal differentiation. Deletion of APC in adult neural
329 stem cells can exhaust the germinal zone and disturb differentiation and migration of neuroblasts
330 in the olfactory bulb (Imura et al., 2010). Our results indicated a serious depletion of *APC* transcript
331 level in the CuNP treatment (Table 1 and Fig. 4A). The reduced transcript abundances of *TCF7L2*
332 and *APC*, which are involved in the positive and negative regulation of Wnt/ β -catenin pathway,
333 respectively, suggests that neurogenesis was disrupted in the CuNP-treated olfactory mucosa. In
334 contrast to the CuNP treatment, there was a significant increase in the mRNA of *APC* in the Cu^{2+}
335 treatment (Table 1). These data suggest that CuNPs and Cu^{2+} distinctly influenced neurogenesis-
336 related processes in olfactory mucosa.

337 **Effect of CuNPs and Cu^{2+} on transcription factors associated with olfactory** 338 **neurogenesis**

339 Transcription factors (TFs) play critical roles in olfactory neuroregeneration (Nicolay et
340 al., 2006; Shetty et al., 2005). In each stage of neurogenesis, specific TFs are activated to mediate
341 and regulate differentiation in the olfactory mucosa. One of the key transcription factors involved

342 in olfactory epithelium development and neuroregeneration is PAX6 (Collinson et al., 2003; Davis
343 and Reed, 1996; Suzuki et al., 2015). The expression of PAX6 was reported in proliferating GBCs
344 in normal and lesioned olfactory epithelium of adult rat (Guo et al., 2010). Deletion of PAX6 in
345 HBCs has resulted in a thinner olfactory epithelial layer with reduced numbers of OSNs in mice
346 (Suzuki et al., 2015). In our study, we observed a 6-fold reduction in the expression of *PAX6*
347 following exposure to CuNPs (Table 1). A previous study also demonstrated that the PAX6 protein
348 expression was reduced in the brain of zebrafish embryos that were exposed to copper oxide
349 nanoparticles (Xu et al., 2017). PAX6 has been shown as a downstream target of the β -catenin-
350 TCF transcriptional complex in the Wnt/ β -catenin pathway; the β -catenin-TCF complex binds to
351 the PAX6 promoter and induces its expression (Gan et al., 2014). Given that the expression of
352 *TCF7L2* was severely repressed in the CuNP treatment, and the reduced expression of *PAX6*, the
353 observed reduction of neurogenesis is plausible in CuNP-exposed olfactory mucosa. Additionally,
354 the expression of *Lhx2* — a transcription factor engaged in the formation of mature OSNs
355 (Berghard et al., 2012; Kolterud et al., 2004) — was also downregulated following exposure to
356 CuNPs (Table 1). Another downregulated TF in the CuNP treatment is *GATA3*, which is an
357 essential TF to initiate stem cells proliferation in adult zebrafish brain (Kizil et al., 2012). The
358 downregulated expression of neurogenesis-related TFs suggested neuroregeneration was impaired
359 in the CuNP treatment.

360 In contrast to the CuNP-exposed fish, a number of TFs that regulate neurogenesis were
361 significantly upregulated following the exposure to Cu^{2+} . For instance, the expression of both
362 *PAX6* and *Lhx2* transcription factors were increased in the olfactory mucosa of the Cu^{2+} -exposed
363 fish (Table 1). Besides the *PAX6* and *Lhx2*, which belong to the homeobox genes, the expression
364 of two other genes from this group, *PBX1* and *OTX1*, were also upregulated (Table 1). The

365 transcriptional activity of both PBX1 (Grebbin and Schulte, 2017) and OTX1 (Heron et al., 2013;
366 Pirrone et al., 2017) regulate neuroregeneration in the olfactory mucosa. Another neurogenesis
367 master TF is *SOX2* (Sokpor et al., 2018), which was significantly induced by Cu^{2+} (Table 1). In
368 the absence of *SOX2* in HBCs, while the formation of a neuronal lineage was inhibited, the
369 production of non-neural (i.e., sustentacular) cells was not affected. Hence, the regeneration of
370 OSNs relies on *SOX2* activity in an injured olfactory epithelium (Gadye et al., 2017). Zinc finger
371 transcription factor *SP8*, which is involved with the development of olfactory epithelium and the
372 olfactory bulb (Kasberg et al., 2013; Waclaw et al., 2006), was also upregulated in the Cu^{2+}
373 treatment (Table 1). The induced gene expression of these neurogenesis-related TFs suggested that
374 neuroregeneration could be initiated in Cu^{2+} -treated olfactory mucosa.

375 **Effect of CuNPs on axonogenesis in the olfactory mucosa**

376 Axonogenesis is an important stage of neural development that ultimately builds a
377 functional connection between new neurons and target cells. In the peripheral nervous system,
378 axonal regeneration mediates functional recovery after injury (He and Jin, 2016). When axon
379 regeneration is initiated, the axon outgrowth will be guided to the olfactory bulb. Following the
380 axons' exit from the olfactory epithelium to the lamina propria, OECs wrap the axons, promote
381 axonal projection, and guide the growth cone to the olfactory bulb (Su and He, 2010). The OECs
382 produce many signaling cues, including growth factors and cell adhesion molecules which
383 facilitate axon regeneration (Roet and Verhaagen, 2014). Following exposure to CuNPs, the OECs
384 altered the olfactory lamina propria microenvironment mostly in favour of axon regeneration. In
385 fact, the expression of neurite outgrowth promoters, which are secreted from OECs, including
386 *SERPINE1*, *SPARC*, *ADAMTS1*, *FGFR2*, *MSLN*, and *FINC* (Lin et al., 2019; Roet et al., 2013),
387 were upregulated (Table 1). However, the expression of two cell adhesion molecules (i.e., *NCAMI*

388 and *CDH2* (a.k.a., *N-CAD*)), which can be produced by OEC to promote the axon outgrowth
389 (Rigby et al., 2020), were significantly decreased in the CuNP-exposed fish (Table 1). These cell
390 adhesion molecules, which are expressed at the surface of OECs, facilitate the attachment of axon
391 growth cones to the migrating OECs moving toward olfactory bulb (Rigby et al., 2020). In addition
392 to the OEC-derived signaling molecules, axon development is also regulated by intrinsic signals
393 (He and Jin, 2016; Mahar and Cavalli, 2018). For instance, the expression of *NTN1* (Astic et al.,
394 2002; Lakhina et al., 2012), *EPHA4* (John et al., 2002), *β 3GNT1* (Henion et al., 2005), which are
395 all involved in axonal pathfinding, was upregulated following exposure to CuNPs (Table 1). These
396 data revealed that axonogenesis regulators endeavor to repair the axonal impairment that may have
397 been induced by CuNPs.

398 Neurons are highly polarized (i.e., asymmetric) cells which usually have a single long axon.
399 Polarity signaling pathways in the axon establish asymmetry in growth cones and control the
400 direction of axon growth (Zou, 2012, 2020). Axon polarity during development and regeneration
401 is regulated by signaling molecules and intracellular mechanisms which are actively interacting to
402 mediate polarity (Arimura and Kaibuchi, 2007; Stone et al., 2010). The non-canonical Wnt/planar
403 cell polarity (PCP) pathway plays a crucial role in regulating epithelial cells' polarity and axonal
404 growth cone guidance (Zou, 2020). In the PCP pathway, the Wnt ligand will bind to its receptor
405 and induce a cascade of events that ultimately activates the JNK pathway (Winter et al., 2001;
406 Zhang et al., 2012). The JNK signaling pathway regulates the expression of axonal regeneration
407 and polarity related genes (Hirai et al., 2011; Kawasaki et al., 2018; Stone et al., 2010). The
408 expression of *JUN*, which is a TF involved in JNK pathway, was significantly downregulated in
409 the CuNP treatment (Table 1). Moreover, there is molecular crosstalk between PCP and other
410 pathways driving axonal polarity, including the PAR complex (aPKC-PAR6-Par3) (Chuykin et

411 al., 2018; Zou, 2012). The interaction of PCP and PAR will increase axonal polarity. The transcript
412 abundance of *PAR3*, which serves as one key mediator of the PAR complex, was diminished
413 following exposure to CuNPs (Table 1). These data indicated that polarity mechanisms involved
414 in axonogenesis may be impaired by CuNPs.

415 Regulating the expression of axonal sprouting and guidance genes is a key step in axon
416 regeneration (He and Jin, 2016; McIntyre et al., 2010). In this study, the upregulated extrinsic and
417 intrinsic axon regrowth and guidance genes may prime the olfactory neuronal axons to regenerate
418 following exposure to CuNPs. Nevertheless, the reduction of cell adhesion molecules (i.e., *NCAMI*
419 and *CDH2*) and polarity regulating genes (i.e., *JUN* and *PAR3*) transcript levels may limit the
420 axonal outgrowth competency in the CuNP treatment. Further investigations are required to
421 determine if axon regeneration is initiated in the CuNP treatment.

422 **Effect of Cu²⁺ on axonogenesis in the olfactory mucosa**

423 In the Cu²⁺ treatment, *MSLN* was the only altered OEC-derived gene that was significantly
424 upregulated. The *MSLN* is a glycoprotein that is produced by OECs to make the extracellular
425 matrix suitable for axon growth (Roet et al., 2013). Although the OEC-driven axonogenesis was
426 induced more by CuNPs than Cu²⁺, the transcript abundances of a number of intrinsic regulators
427 of axonogenesis were increased in the Cu²⁺-exposed olfactory mucosa. Axonal outgrowth is highly
428 dependent on intact intracellular trafficking to deliver essential cargo to the growing axon
429 (McCormick and Gupton, 2020). A multi-subunit protein, BLOC1, is an important component of
430 the cell membrane and of vesicular trafficking in the developing axon (McCormick and Gupton,
431 2020). Neurons deficient in BLOC1 demonstrated insufficient neurite outgrowth in the
432 hippocampus (Ghiani et al., 2010). The expression of BLOC1 subunit 1 (*BLOC1S1*) was
433 significantly increased in the Cu²⁺ treatment (Table 1). Additionally, two endocytic accessory

434 proteins, *EPS15L1* (a.k.a., *EPS15R*) and *CALM*, which participate in intracellular trafficking
435 (Moore and Baleja, 2012), were highly transcribed in the Cu²⁺ treatment. The expression of
436 vesicular trafficking genes, including *RAB3A* and *RAB10* which regulate synaptic vesicle cycling
437 (Pavlos et al., 2010), were also increased in the Cu²⁺-exposed fish.

438 In order to have functional neural wiring in the olfactory system, the polarity and
439 pathfinding mediators must accurately guide the neurons' axons to the olfactory bulb. One of the
440 axonal pathfinding genes is *ROBO2*, which was upregulated in the Cu²⁺ treatment (Table 1).
441 Previous studies have suggested that the knockout of *ROBO2* in the OSNs can lead to axonal
442 mistargeting in the OB (Cho et al., 2007; Miyasaka et al., 2005). Moreover, the expression of *PAR3*
443 was significantly increased in Cu²⁺-exposed mucosal cells (Table 1). Another important polarity
444 regulation protein in the axonal growth cone is a guanine nucleotide exchange factor named
445 *TIAM1* (Montenegro-Venegas et al., 2010). The expression of *TIAM1* was also upregulated
446 following the Cu²⁺ exposure (Table 1). The PAR complex (specifically *PAR3*) has been reported
447 to form a complex with *TIAM1* and regulates neural polarization (Zhang and Macara, 2006). The
448 gene expression of two microtubule-associated proteins involved in axon formation and
449 polarization, *MAP1A* and *MAP1B* (Halpain and Dehmelt, 2006), were increased in the Cu²⁺
450 treatment (Table 1). The *MAP1B* plays a role in axonal elongation and neural migration (Takei et
451 al., 2000). In addition, the interaction of *MAP1B* and *TIAM1* is fundamental to regulating polarity
452 in axonogenesis (Montenegro-Venegas et al., 2010). Furthermore, *TRIM46*, which organizes
453 microtubules trafficking and orientation and, consequently, regulates polarity in axons, was
454 upregulated in the Cu²⁺ treatment (Rao et al., 2017). This upregulation of of axonogenesis-related
455 gene transcripts in the Cu²⁺-exposed olfactory mucosa revealed that the intrinsic neural
456 mechanisms were in play to fulfill the axonal outgrowth requirements in the Cu²⁺-treated fish.

457 **Conclusions**

458 This study provides insight into impacts of CuNPs and Cu²⁺ on the neural repair
459 mechanisms in rainbow trout olfactory mucosa. The transcript profile of olfactory mucosa
460 indicated that CuNPs had more inhibitory influences on neuroregeneration mechanisms relative to
461 axonal repair mechanisms. The transcripts of many extrinsic and intrinsic neurogenesis regulators
462 were reduced by CuNPs. The inhibition of neuroregeneration reduces the likelihood of olfactory
463 recovery in CuNP-exposed fish. Nonetheless, exposure to CuNPs induced molecular responses
464 that mostly promote axon regeneration in olfactory mucosa. The functionality of axonal repair in
465 the CuNP treatment needs to be investigated further. In the Cu²⁺ treatment, the upregulated
466 transcripts of many genes directing neurogenesis and axonogenesis reflects that both reparative
467 mechanisms were activated. These results can explain the previously observed functional recovery
468 of Cu²⁺-exposed OSNs over the 96-h exposure period in rainbow trout. Given that CuNPs may
469 impair the OSN function and reconstitution, development of a water quality criterion to protect
470 fish against CuNPs is warranted.

471 **Acknowledgments**

472 The authors would like to thank the University of Lethbridge Aquatic Research facility
473 staff Dr. Shamsuddin Mamun and Holly Shepherd for taking care of study fish.

474

475

476

477

478

- 480 Aegerter, S., Jalabert, B., Bobe, J., 2005. Large scale real-time PCR analysis of mRNA abundance
481 in rainbow trout eggs in relationship with egg quality and post-ovulatory ageing. *Molecular*
482 *Reproduction and Development: Incorporating Gamete Research* 72, 377-385.
- 483 Agarwal, H., Nakara, A., Shanmugam, V.K., 2019. Anti-inflammatory mechanism of various
484 metal and metal oxide nanoparticles synthesized using plant extracts: A review. *Biomedicine &*
485 *Pharmacotherapy* 109, 2561-2572.
- 486 Andrews, S., 2020. FastQC: a quality control tool for high throughput sequence data. 2010.
- 487 Arimura, N., Kaibuchi, K., 2007. Neuronal polarity: from extracellular signals to intracellular
488 mechanisms. *Nature Reviews Neuroscience* 8, 194-205.
- 489 Ashraf, P.M., Sasikala, K., Thomas, S.N., Edwin, L., 2017. Biofouling resistant polyethylene cage
490 aquaculture nettings: A new approach using polyaniline and nano copper oxide. *Arabian Journal*
491 *of Chemistry* 13, 875-882.
- 492 Astic, L., Pellier-Monnin, V., Saucier, D., Charrier, C., Mehlen, P., 2002. Expression of netrin-1
493 and netrin-1 receptor, DCC, in the rat olfactory nerve pathway during development and axonal
494 regeneration. *Neuroscience* 109, 643-656.
- 495 Bengoa-Vergniory, N., Kypta, R.M., 2015. Canonical and noncanonical Wnt signaling in neural
496 stem/progenitor cells. *Cellular and Molecular Life Sciences* 72, 4157-4172.
- 497 Berghard, A., Hägglund, A.C., Bohm, S., Carlsson, L., 2012. Lhx2-dependent specification of
498 olfactory sensory neurons is required for successful integration of olfactory, vomeronasal, and
499 GnRH neurons. *The FASEB Journal* 26, 3464-3472.
- 500 Bols, N.C., Brubacher, J.L., Ganassin, R.C., Lee, L.E., 2001. Ecotoxicology and innate immunity
501 in fish. *Developmental & Comparative Immunology* 25, 853-873.
- 502 Chang, S.Y., Glezer, I., 2018. The balance between efficient anti-inflammatory treatment and
503 neuronal regeneration in the olfactory epithelium. *Neural Regeneration Research* 13, 1711.
- 504 Chari, N., Felix, L., Davoodbasha, M., Ali, A.S., Nooruddin, T., 2017. In vitro and in vivo
505 antibiofilm effect of copper nanoparticles against aquaculture pathogens. *Biocatalysis and*
506 *Agricultural Biotechnology* 10, 336-341.
- 507 Chen, M., Reed, R.R., Lane, A.P., 2017. Acute inflammation regulates neuroregeneration through
508 the NF- κ B pathway in olfactory epithelium. *Proceedings of the National Academy of Sciences*
509 114, 8089-8094.
- 510 Chen, M., Reed, R.R., Lane, A.P., 2019. Chronic inflammation directs an olfactory stem cell
511 functional switch from neuroregeneration to immune defense. *Cell Stem Cell* 25, 501-513. e505.
- 512 Chen, M., Tian, S., Yang, X., Lane, A.P., Reed, R.R., Liu, H., 2014. Wnt-responsive Lgr5+
513 globose basal cells function as multipotent olfactory epithelium progenitor cells. *Journal of*
514 *Neuroscience* 34, 8268-8276.
- 515 Cho, J.H., Lépine, M., Andrews, W., Parnavelas, J., Cloutier, J.-F., 2007. Requirement for Slit-1
516 and Robo-2 in zonal segregation of olfactory sensory neuron axons in the main olfactory bulb.
517 *Journal of Neuroscience* 27, 9094-9104.

518 Choi, R., Goldstein, B.J., 2018. Olfactory epithelium: cells, clinical disorders, and insights from
519 an adult stem cell niche. *Laryngoscope Investigative Otolaryngology* 3, 35-42.

520 Chuykin, I., Ossipova, O., Sokol, S.Y., 2018. Par3 interacts with Prickle3 to generate apical PCP
521 complexes in the vertebrate neural plate. *Elife* 7, e37881.

522 Collinson, J.M., Quinn, J.C., Hill, R.E., West, J.D., 2003. The roles of Pax6 in the cornea, retina,
523 and olfactory epithelium of the developing mouse embryo. *Developmental Biology* 255, 303-312.

524 Crisafulli, U., Xavier, A.M., dos Santos, F.B., Cambiaghi, T.D., Chang, S.Y., Porcionatto, M.,
525 Castilho, B.A., Malnic, B., Glezer, I., 2018. Topical dexamethasone administration impairs protein
526 synthesis and neuronal regeneration in the olfactory epithelium. *Frontiers in Molecular*
527 *Neuroscience* 11, 50.

528 Davis, J.A., Reed, R.R., 1996. Role of Olf-1 and Pax-6 transcription factors in neurodevelopment.
529 *Journal of Neuroscience* 16, 5082-5094.

530 de Rivero Vaccari, J.P., Dietrich, W.D., Keane, R.W., 2014. Activation and regulation of cellular
531 inflammasomes: gaps in our knowledge for central nervous system injury. *Journal of Cerebral*
532 *Blood Flow & Metabolism* 34, 369-375.

533 Dobin, A., Davis, C.A., Schlesinger, F., Drenkow, J., Zaleski, C., Jha, S., Batut, P., Chaisson, M.,
534 Gingeras, T.R., 2013. STAR: ultrafast universal RNA-seq aligner. *Bioinformatics* 29, 15-21.

535 El Basuini, M., El-Hais, A., Dawood, M., Abou-Zeid, A.S., El-Damrawy, S., Khalafalla, M.S.,
536 Koshio, S., Ishikawa, M., Dossou, S., 2017. Effects of dietary copper nanoparticles and vitamin C
537 supplementations on growth performance, immune response and stress resistance of red sea bream,
538 *Pagrus major*. *Aquaculture Nutrition* 23, 1329-1340.

539 Fletcher, R.B., Das, D., Gadye, L., Street, K.N., Baudhuin, A., Wagner, A., Cole, M.B., Flores,
540 Q., Choi, Y.G., Yosef, N., 2017. Deconstructing olfactory stem cell trajectories at single-cell
541 resolution. *Cell stem cell* 20, 817-830. e818.

542 Gadye, L., Das, D., Sanchez, M.A., Street, K., Baudhuin, A., Wagner, A., Cole, M.B., Choi, Y.G.,
543 Yosef, N., Purdom, E., 2017. Injury activates transient olfactory stem cell states with diverse
544 lineage capacities. *Cell Stem Cell* 21, 775-790. e779.

545 Gan, Q., Lee, A., Suzuki, R., Yamagami, T., Stokes, A., Nguyen, B.C., Pleasure, D., Wang, J.,
546 Chen, H.W., Zhou, C.J., 2014. Pax6 mediates ss-catenin signaling for self-renewal and
547 neurogenesis by neocortical radial glial stem cells. *Stem Cells* 32, 45-58.

548 Gharagozloo, M., Mahvelati, T.M., Imbeault, E., Gris, P., Zerif, E., Bobbala, D., Ilangumaran, S.,
549 Amrani, A., Gris, D., 2015. The nod-like receptor, Nlrp12, plays an anti-inflammatory role in
550 experimental autoimmune encephalomyelitis. *Journal of Neuroinflammation* 12, 1-13.

551 Ghiani, C., Starcevic, M., Rodriguez-Fernandez, I., Nazarian, R., Cheli, V., Chan, L., Malvar, J.,
552 De Vellis, J., Sabatti, C., Dell'Angelica, E., 2010. The dysbindin-containing complex (BLOC-1)
553 in brain: developmental regulation, interaction with SNARE proteins and role in neurite
554 outgrowth. *Molecular Psychiatry* 15, 204-215.

555 Götz, S., García-Gómez, J.M., Terol, J., Williams, T.D., Nagaraj, S.H., Nueda, M.J., Robles, M.,
556 Talón, M., Dopazo, J., Conesa, A., 2008. High-throughput functional annotation and data mining
557 with the Blast2GO suite. *Nucleic Acids Research* 36, 3420-3435.

558 Graziadei, G.M., Graziadei, P.P.C., 1979. Neurogenesis and neuron regeneration in the olfactory
559 system of mammals. II. Degeneration and reconstitution of the olfactory sensory neurons after
560 axotomy. *Journal of Neurocytology* 8, 197-213.

561 Grebbin, B.M., Schulte, D., 2017. PBX1 as pioneer factor: a case still open. *Frontiers in Cell and*
562 *Developmental Biology* 5, 9.

563 Guo, Z., Packard, A., Krolewski, R.C., Harris, M.T., Manglapus, G.L., Schwob, J.E., 2010.
564 Expression of pax6 and sox2 in adult olfactory epithelium. *Journal of Comparative Neurology* 518,
565 4395-4418.

566 Halpain, S., Dehmelt, L., 2006. The MAP1 family of microtubule-associated proteins. *Genome*
567 *Biology* 7, 224.

568 Hasegawa, T., Hall, C.J., Crosier, P.S., Abe, G., Kawakami, K., Kudo, A., Kawakami, A., 2017.
569 Transient inflammatory response mediated by interleukin-1 β is required for proper regeneration in
570 zebrafish fin fold. *Elife* 6, e22716.

571 He, Z., Jin, Y., 2016. Intrinsic control of axon regeneration. *Neuron* 90, 437-451.

572 Hegg, C.C., Irwin, M., Lucero, M.T., 2009. Calcium store-mediated signaling in sustentacular cells
573 of the mouse olfactory epithelium. *Glia* 57, 634-644.

574 Henion, T.R., Raitcheva, D., Grosholz, R., Biellmann, F., Skarnes, W.C., Hennet, T., Schwarting,
575 G.A., 2005. β 1, 3-N-acetylglucosaminyltransferase 1 glycosylation is required for axon
576 pathfinding by olfactory sensory neurons. *Journal of Neuroscience* 25, 1894-1903.

577 Heron, P.M., Stromberg, A.J., Breheny, P., McClintock, T.S., 2013. Molecular events in the cell
578 types of the olfactory epithelium during adult neurogenesis. *Molecular Brain* 6, 49.

579 Hirai, S.-i., Banba, Y., Satake, T., Ohno, S., 2011. Axon Formation in Neocortical Neurons
580 Depends on Stage-Specific Regulation of Microtubule Stability by the Dual Leucine Zipper
581 Kinase-c-Jun N-Terminal Kinase Pathway. *Journal of Neuroscience* 31, 6468-6480.

582 Imura, T., Wang, X., Noda, T., Sofroniew, M.V., Fushiki, S., 2010. Adenomatous polyposis coli
583 is essential for both neuronal differentiation and maintenance of adult neural stem cells in
584 subventricular zone and hippocampus. *Stem Cells* 28, 2053-2064.

585 John, J.A.S., Pasquale, E.B., Key, B., 2002. EphA receptors and ephrin-A ligands exhibit highly
586 regulated spatial and temporal expression patterns in the developing olfactory system.
587 *Developmental Brain Research* 138, 1-14.

588 Kasberg, A.D., Brunskill, E.W., Potter, S.S., 2013. SP8 regulates signaling centers during
589 craniofacial development. *Developmental Biology* 381, 312-323.

590 Kawasaki, A., Okada, M., Tamada, A., Okuda, S., Nozumi, M., Ito, Y., Kobayashi, D., Yamasaki,
591 T., Yokoyama, R., Shibata, T., 2018. Growth cone phosphoproteomics reveals that GAP-43
592 phosphorylated by JNK is a marker of axon growth and regeneration. *iScience* 4, 190-203.

593 Kermen, F., Franco, L.M., Wyatt, C., Yaksi, E., 2013. Neural circuits mediating olfactory-driven
594 behavior in fish. *Frontiers in Neural Circuits* 7, 62.

595 Kizil, C., Kyritsis, N., Dudczig, S., Kroehne, V., Freudenreich, D., Kaslin, J., Brand, M., 2012.
596 Regenerative neurogenesis from neural progenitor cells requires injury-induced expression of
597 Gata3. *Developmental Cell* 23, 1230-1237.

598 Kolterud, Å., Alenius, M., Carlsson, L., Bohm, S., 2004. The Lim homeobox gene Lhx2 is required
599 for olfactory sensory neuron identity. *Development* 131, 5319-5326.

600 Kyritsis, N., Kizil, C., Zocher, S., Kroehne, V., Kaslin, J., Freudenreich, D., Iltzsche, A., Brand,
601 M., 2012. Acute inflammation initiates the regenerative response in the adult zebrafish brain.
602 *Science* 338, 1353-1356.

603 Laberge, F., Hara, T.J., 2001. Neurobiology of fish olfaction: a review. *Brain Research Reviews*
604 36, 46-59.

605 Lakhina, V., Marcaccio, C.L., Shao, X., Lush, M.E., Jain, R.A., Fujimoto, E., Bonkowsky, J.L.,
606 Granato, M., Raper, J.A., 2012. Netrin/DCC signaling guides olfactory sensory axons to their
607 correct location in the olfactory bulb. *Journal of Neuroscience* 32, 4440-4456.

608 Lin, N., Dong, X.J., Wang, T.Y., He, W.J., Wei, J., Wu, H.Y., Wang, T.H., 2019. Characteristics
609 of olfactory ensheathing cells and microarray analysis in *Tupaia belangeri* (Wagner, 1841).
610 *Molecular Medicine Reports* 20, 1819-1825.

611 Liu, T., Zhang, L., Joo, D., Sun, S.-C., 2017. NF- κ B signaling in inflammation. *Signal*
612 *Transduction and Targeted Therapy* 2, 1-9.

613 Love, M.I., Huber, W., Anders, S., 2014. Moderated estimation of fold change and dispersion for
614 RNA-seq data with DESeq2. *Genome Biology* 15, 550.

615 Ma, E.Y., Heffern, K., Cheresch, J., Gallagher, E.P., 2018. Differential copper-induced death and
616 regeneration of olfactory sensory neuron populations and neurobehavioral function in larval
617 zebrafish. *Neurotoxicology* 69, 141-151.

618 Mahar, M., Cavalli, V., 2018. Intrinsic mechanisms of neuronal axon regeneration. *Nature*
619 *Reviews Neuroscience* 19, 323-337.

620 Malhotra, N., Ger, T.-R., Uapipatanakul, B., Huang, J.-C., Chen, K.H.-C., Hsiao, C.-D., 2020.
621 Review of Copper and Copper Nanoparticle Toxicity in Fish. *Nanomaterials* 10, 1126.

622 McCormick, L.E., Gupton, S.L., 2020. Mechanistic advances in axon pathfinding. *Current Opinion*
623 *in Cell Biology* 63, 11-19.

624 McIntyre, J.C., Titlow, W.B., McClintock, T.S., 2010. Axon growth and guidance genes identify
625 nascent, immature, and mature olfactory sensory neurons. *Journal of Neuroscience Research* 88,
626 3243-3256.

627 Miyasaka, N., Sato, Y., Yeo, S.-Y., Hutson, L.D., Chien, C.-B., Okamoto, H., Yoshihara, Y., 2005.
628 Robo2 is required for establishment of a precise glomerular map in the zebrafish olfactory system.
629 *Development* 132, 1283-1293.

630 Montenegro-Venegas, C., Tortosa, E., Rosso, S., Peretti, D., Bollati, F., Bisbal, M., Jausoro, I.,
631 Avila, J., Cáceres, A., Gonzalez-Billault, C., 2010. MAP1B regulates axonal development by
632 modulating Rho-GTPase Rac1 activity. *Molecular Biology of the Cell* 21, 3518-3528.

633 Moore, F.B., Baleja, J.D., 2012. Molecular remodeling mechanisms of the neural somatodendritic
634 compartment. *Biochimica et Biophysica Acta (BBA)-Molecular Cell Research* 1823, 1720-1730.

635 Nicolay, D.J., Doucette, J.R., Nazarali, A.J., 2006. Transcriptional regulation of neurogenesis in
636 the olfactory epithelium. *Cellular and Molecular Neurobiology* 26, 801-819.

637 Pasparakis, M., 2009. Regulation of tissue homeostasis by NF- κ B signalling: implications for
638 inflammatory diseases. *Nature Reviews Immunology* 9, 778-788.

639 Pavlos, N.J., Grønberg, M., Riedel, D., Chua, J.J., Boyken, J., Kloepper, T.H., Urlaub, H., Rizzoli,
640 S.O., Jahn, R., 2010. Quantitative analysis of synaptic vesicle Rabs uncovers distinct yet
641 overlapping roles for Rab3a and Rab27b in Ca²⁺-triggered exocytosis. *Journal of Neuroscience*
642 30, 13441-13453.

643 Pertea, M., Pertea, G.M., Antonescu, C.M., Chang, T.-C., Mendell, J.T., Salzberg, S.L., 2015.
644 StringTie enables improved reconstruction of a transcriptome from RNA-seq reads. *Nature*
645 *Biotechnology* 33, 290-295.

646 Pfaffl, M.W., 2001. A new mathematical model for relative quantification in real-time RT-PCR.
647 *Nucleic Acids Research* 29, e45-e45.

648 Pirrone, C., Chiaravalli, A.M., Marando, A., Conti, A., Rainero, A., Pistochini, A., Curto, F.L.,
649 Pasquali, F., Castelnuovo, P., Capella, C., 2017. OTX1 and OTX2 as possible molecular markers
650 of sinonasal carcinomas and olfactory neuroblastomas. *European Journal of Histochemistry: EJH*
651 61.

652 Polakof, S., Médale, F., Skiba-Cassy, S., Corraze, G., Panserat, S., 2010. Molecular regulation of
653 lipid metabolism in liver and muscle of rainbow trout subjected to acute and chronic insulin
654 treatments. *Domestic Animal Endocrinology* 39, 26-33.

655 Pu, Y., Liu, H., Xu, H., Liu, H., Cheng, Y., Chen, X., Xu, W., Xu, Y., Fan, J., 2018. IL-1 β promotes
656 the migration of olfactory epithelium neural stem cells through activating matrix metalloproteinase
657 expressions. *Pathology-Research and Practice* 214, 1210-1217.

658 R Core Team, 2019. A language and environment for statistical computing. R Foundation for
659 Statistical Computing, Vienna, Austria2014, in: Team, R.C. (Ed.).

660 Rao, A.N., Patil, A., Black, M.M., Craig, E.M., Myers, K.A., Yeung, H.T., Baas, P.W., 2017.
661 Cytoplasmic dynein transports axonal microtubules in a polarity-sorting manner. *Cell reports* 19,
662 2210-2219.

663 Razmara, P., Imbery, J.J., Koide, E., Helbing, C.C., Wiseman, S.B., Gauthier, P.T., Bray, D.F.,
664 Needham, M., Haight, T., Zovoilis, A., 2021. Mechanism of copper nanoparticle toxicity in
665 rainbow trout olfactory mucosa. *Environmental Pollution* 284, 117141.

666 Razmara, P., Lari, E., Mohaddes, E., Zhang, Y., Goss, G.G., Pyle, G.G., 2019. The effect of copper
667 nanoparticles on olfaction in rainbow trout (*Oncorhynchus mykiss*). *Environmental Science: Nano*
668 6, 2094-2104.

669 Razmara, P., Pyle, G.G., 2022. Recovery of rainbow trout olfactory function following exposure
670 to copper nanoparticles and copper ions. *Aquatic Toxicology* 245, 106109.

671 Rigby, M.J., Gomez, T.M., Puglielli, L., 2020. Glial Cell-Axonal Growth Cone Interactions in
672 Neurodevelopment and Regeneration. *Frontiers in Neuroscience* 14, 203.

673 Roet, K.C., Franssen, E.H., de Bree, F.M., Essing, A.H., Zijlstra, S.-J.J., Fagoe, N.D., Eggink,
674 H.M., Eggers, R., Smit, A.B., van Kesteren, R.E., 2013. A multilevel screening strategy defines a
675 molecular fingerprint of proregenerative olfactory ensheathing cells and identifies SCARB2, a
676 protein that improves regenerative sprouting of injured sensory spinal axons. *Journal of*
677 *Neuroscience* 33, 11116-11135.

678 Roet, K.C., Verhaagen, J., 2014. Understanding the neural repair-promoting properties of olfactory
679 ensheathing cells. *Experimental Neurology* 261, 594-609.

680 Rossner, P., Vrbova, K., Rossnerova, A., Zavodna, T., Milcova, A., Klema, J., Vecera, Z.,
681 Mikuska, P., Coufalik, P., Capka, L., 2020. Gene Expression and Epigenetic Changes in Mice
682 Following Inhalation of Copper (II) Oxide Nanoparticles. *Nanomaterials* 10, 550.

683 Roy, D., Ghosh, D., Mandal, D.K., 2013. Cadmium induced histopathology in the olfactory
684 epithelium of a snakehead fish, *Channa punctatus* (Bloch). *International Journal of Aquatic
685 Biology* 1, 221-227.

686 Sharma, D., Malik, A., Guy, C., Vogel, P., Kanneganti, T.-D., 2019. TNF/TNFR axis promotes
687 pyrin inflammasome activation and distinctly modulates pyrin inflammasomopathy. *The Journal
688 of Clinical Investigation* 129, 150-162.

689 Shetty, R.S., Bose, S.C., Nickell, M.D., McIntyre, J.C., Hardin, D.H., Harris, A.M., McClintock,
690 T.S., 2005. Transcriptional changes during neuronal death and replacement in the olfactory
691 epithelium. *Molecular and Cellular Neuroscience* 30, 90-107.

692 Shimizu, N., Kawakami, K., Ishitani, T., 2012. Visualization and exploration of Tcf/Lef function
693 using a highly responsive Wnt/ β -catenin signaling-reporter transgenic zebrafish. *Developmental
694 Biology* 370, 71-85.

695 Sokpor, G., Abbas, E., Rosenbusch, J., Staiger, J.F., Tuoc, T., 2018. Transcriptional and epigenetic
696 control of mammalian olfactory epithelium development. *Molecular Neurobiology* 55, 8306-8327.

697 Stone, M.C., Nguyen, M.M., Tao, J., Allender, D.L., Rolls, M.M., 2010. Global up-regulation of
698 microtubule dynamics and polarity reversal during regeneration of an axon from a dendrite.
699 *Molecular Biology of the Cell* 21, 767-777.

700 Su, Z., He, C., 2010. Olfactory ensheathing cells: biology in neural development and regeneration.
701 *Progress in Neurobiology* 92, 517-532.

702 Sun, S.-C., 2011. Non-canonical NF- κ B signaling pathway. *Cell Research* 21, 71-85.

703 Sun, S.-C., 2017. The non-canonical NF- κ B pathway in immunity and inflammation. *Nature
704 Reviews Immunology* 17, 545.

705 Suzuki, J., Sakurai, K., Yamazaki, M., Abe, M., Inada, H., Sakimura, K., Katori, Y., Osumi, N.,
706 2015. Horizontal basal cell-specific deletion of Pax6 impedes recovery of the olfactory
707 neuroepithelium following severe injury. *Stem Cells and Development* 24, 1923-1933.

708 Szymkowicz, D.B., Sims, K.C., Schwendinger, K.L., Tatnall, C.M., Powell, R.R., Bruce, T.F.,
709 Bridges, W.C., Bain, L.J., 2019. Exposure to arsenic during embryogenesis impairs olfactory
710 sensory neuron differentiation and function into adulthood. *Toxicology* 420, 73-84.

711 Tabesh, E., Salimijazi, H., Kharaziha, M., Hejazi, M., 2018. Antibacterial chitosan-copper
712 nanocomposite coatings for biomedical applications. *Materials Today: Proceedings* 5, 15806-
713 15812.

714 Takei, Y., Teng, J., Harada, A., Hirokawa, N., 2000. Defects in axonal elongation and neuronal
715 migration in mice with disrupted tau and map1b genes. *The Journal of Cell Biology* 150, 989-
716 1000.

717 Thiruvengadam, M., Chung, I.-M., Gomathi, T., Ansari, M.A., Khanna, V.G., Babu, V.,
718 Rajakumar, G., 2019. Synthesis, characterization and pharmacological potential of green
719 synthesized copper nanoparticles. *Bioprocess and Biosystems Engineering* 42, 1769-1777.

720 Tilton, F., Tilton, S.C., Bammler, T.K., Beyer, R., Farin, F., Stapleton, P.L., Gallagher, E.P., 2008.
721 Transcriptional biomarkers and mechanisms of copper-induced olfactory injury in zebrafish.
722 *Environmental Science & Technology* 42, 9404-9411.

723 Tsarouchas, T.M., Wehner, D., Cavone, L., Munir, T., Keatinge, M., Lambertus, M., Underhill,
724 A., Barrett, T., Kassapis, E., Ogryzko, N., 2018. Dynamic control of proinflammatory cytokines
725 Il-1 β and Tnf- α by macrophages in zebrafish spinal cord regeneration. *Nature Communications* 9,
726 1-17.

727 Tuncer, S., Fiorillo, M.T., Sorrentino, R., 2014. The multifaceted nature of NLRP12. *Journal of*
728 *Leukocyte Biology* 96, 991-1000.

729 Valiño-Rivas, L., Gonzalez-Lafuente, L., Sanz, A.B., Ruiz-Ortega, M., Ortiz, A., Sanchez-Niño,
730 M.D., 2016. Non-canonical NF κ B activation promotes chemokine expression in podocytes.
731 *Scientific Reports* 6, 28857.

732 Vanti, G.L., Masaphy, S., Kurjogi, M., Chakrasali, S., Nargund, V.B., 2020. Synthesis and
733 application of chitosan-copper nanoparticles on damping off causing plant pathogenic fungi.
734 *International Journal of Biological Macromolecules* 156, 1387-1395.

735 Waclaw, R.R., Allen II, Z.J., Bell, S.M., Erdélyi, F., Szabó, G., Potter, S.S., Campbell, K., 2006.
736 The zinc finger transcription factor Sp8 regulates the generation and diversity of olfactory bulb
737 interneurons. *Neuron* 49, 503-516.

738 Wang, H., Engstrom, A.K., Xia, Z., 2017a. Cadmium impairs the survival and proliferation of
739 cultured adult subventricular neural stem cells through activation of the JNK and p38 MAP
740 kinases. *Toxicology* 380, 30-37.

741 Wang, L., Bammler, T.K., Beyer, R.P., Gallagher, E.P., 2013. Copper-induced deregulation of
742 microRNA expression in the zebrafish olfactory system. *Environmental Science & Technology*
743 47, 7466-7474.

744 Wang, Y., Yang, Q.-W., Yang, Q., Zhou, T., Shi, M.-F., Sun, C.-X., Gao, X.-X., Cheng, Y.-Q.,
745 Cui, X.-G., Sun, Y.-H., 2017b. Cuprous oxide nanoparticles inhibit prostate cancer by attenuating
746 the stemness of cancer cells via inhibition of the Wnt signaling pathway. *International Journal of*
747 *Nanomedicine* 12, 2569.

748 Wang, Y.-Z., Yamagami, T., Gan, Q., Wang, Y., Zhao, T., Hamad, S., Lott, P., Schnittke, N.,
749 Schwob, J.E., Zhou, C.J., 2011. Canonical Wnt signaling promotes the proliferation and
750 neurogenesis of peripheral olfactory stem cells during postnatal development and adult
751 regeneration. *Journal of Cell Science* 124, 1553-1563.

752 Winter, C.G., Wang, B., Ballew, A., Royou, A., Karess, R., Axelrod, J.D., Luo, L., 2001.
753 *Drosophila* Rho-associated kinase (Drok) links Frizzled-mediated planar cell polarity signaling to
754 the actin cytoskeleton. *Cell* 105, 81-91.

755 Xu, J., Zhang, Q., Li, X., Zhan, S., Wang, L., Chen, D., 2017. The effects of copper oxide
756 nanoparticles on dorsoventral patterning, convergent extension, and neural and cardiac
757 development of zebrafish. *Aquatic Toxicology* 188, 130-137.

758 Ye, J., Coulouris, G., Zaretskaya, I., Cutcutache, I., Rozen, S., Madden, T.L., 2012. Primer-
759 BLAST: a tool to design target-specific primers for polymerase chain reaction. BMC
760 Bioinformatics 13, 134.

761 Zhang, H., Macara, I.G., 2006. The polarity protein PAR-3 and TIAM1 cooperate in dendritic
762 spine morphogenesis. Nature Cell biology 8, 227-237.

763 Zhang, Y., Liu, J., Yao, S., Li, F., Xin, L., Lai, M., Bracchi-Ricard, V., Xu, H., Yen, W., Meng,
764 W., 2012. Nuclear factor kappa B signaling initiates early differentiation of neural stem cells. Stem
765 Cells 30, 510-524.

766 Zhou, Y., Wu, S., Liu, F., 2019. High-performance polyimide nanocomposites with
767 polydopamine-coated copper nanoparticles and nanowires for electronic applications. Materials
768 Letters 237, 19-21.

769 Zou, Y., 2012. Does planar cell polarity signaling steer growth cones?, Current topics in
770 developmental biology. Elsevier, pp. 141-160.

771 Zou, Y., 2020. Breaking symmetry—cell polarity signaling pathways in growth cone guidance and
772 synapse formation. Current Opinion in Neurobiology 63, 77-86.

773

774 **Statements and Declarations**

775 **Funding**

776 The current study was supported by an NSERC Discovery Grant (# RGPIN-2015-04492)
777 and a Campus Alberta Innovation Program (CAIP) research chair to GGP.

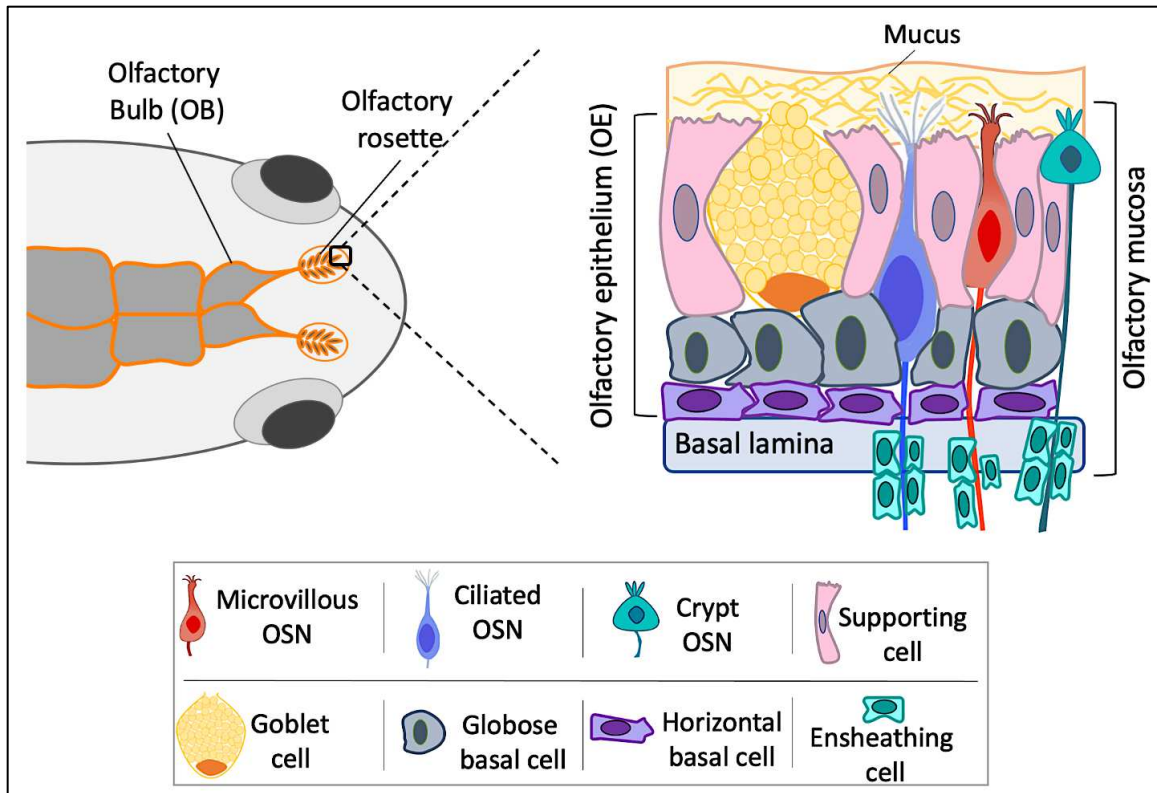
778 **Competing Interests**

779 The authors have no relevant financial or non-financial interests to disclose.

780 **Author Contributions**

781 Both authors contributed to the study conception and design. Material preparation, data
782 collection and analysis were performed by Parastoo Razmara. The first draft of the manuscript was
783 written by Parastoo Razmara, and both authors commented on previous versions of the manuscript.
784 Both authors read and approved the final manuscript

785



786

787

Figure 1. Schematic representation of fish olfactory system. Left drawing shows the position of olfactory system in the dorsal anterior side of the head. Right drawing shows the organization of different types of sensory (i.e., olfactory sensory neurons (OSNs)) and non-sensory cells residing in the olfactory mucosa.

788

789

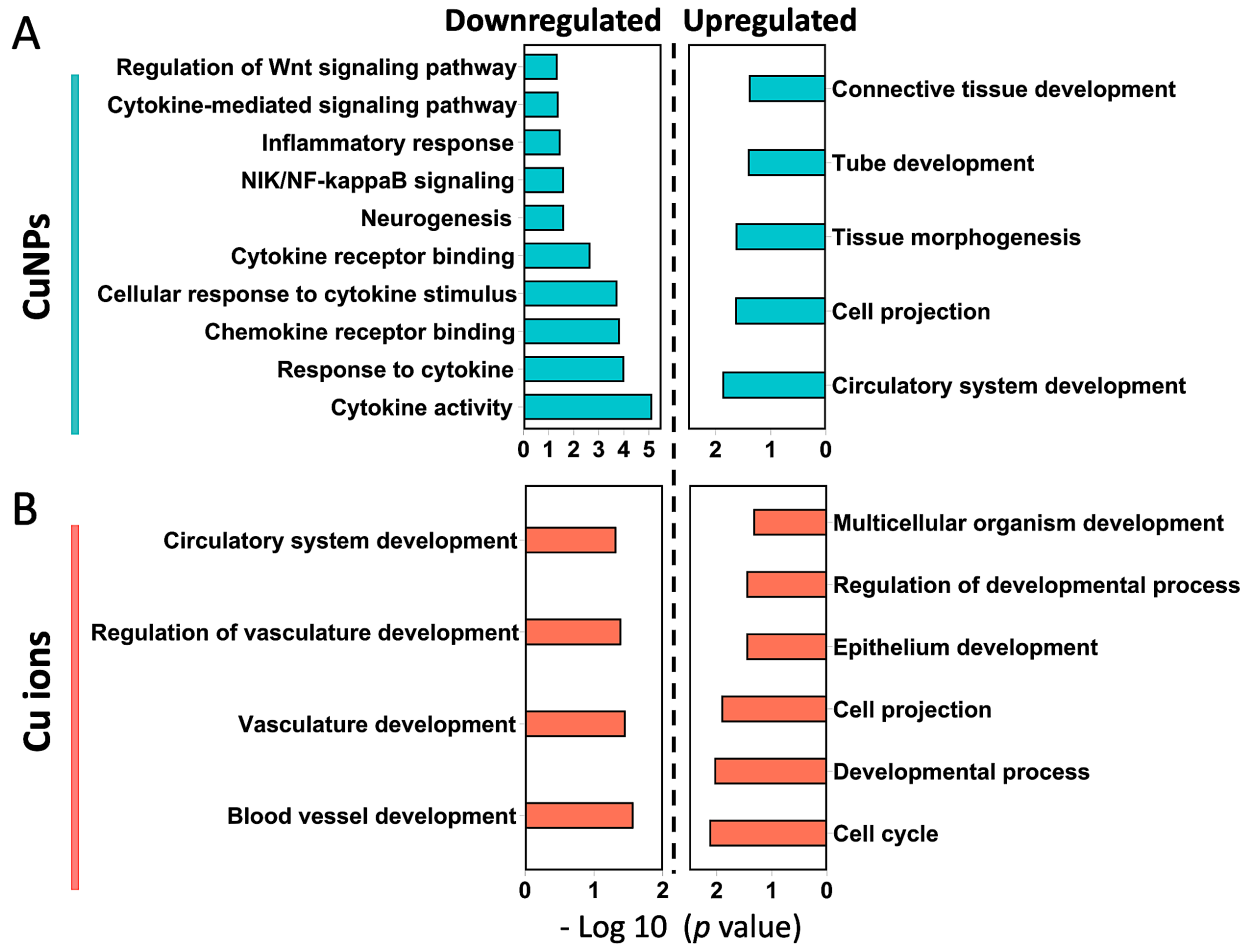
790

791

792

793

794



795

796

797

798

799

800

Figure 2. Over-represented functional GO terms associated with regeneration in CuNP- and Cu²⁺-treated rainbow trout olfactory mucosa. Bar graphs show the enriched GO terms of genes that were significantly upregulated or downregulated in CuNPs (A) and Cu²⁺ (B) treatment. The GO terms ordered according to -Log₁₀ (p value). The p value for each GO term was calculated through Fisher's exact test ($p \leq 0.05$).

801 Table 1. List of differentially expressed genes that regulate repair mechanisms in the rainbow
 802 trout olfactory mucosa following exposure to CuNPs or Cu²⁺. Gene expression was analysed by
 803 RNA-seq. * indicates significant expression relative to the control and “Inf” indicates > 150-fold
 804 change
 805

Biological process	Gene name	Fold change in CuNPs	Fold change in Cu ²⁺
Inflammatory response	Interleukin-1 beta (<i>IL-1β</i>)	0.3 *	0.9
	C-C motif chemokine 4 (<i>CCL4</i>)	0.3 *	0.5
	C-C motif chemokine 19 (<i>CCL19</i>)	0.4 *	0.8
	C-C motif chemokine 20 (<i>CCL20</i>)	0.2 *	0.7
	C-C motif chemokine 25 (<i>CCL25</i>)	0.6 *	1
	Caspase-1 (<i>CASP1</i>)	0.7 *	0.9
	NACHT, LRR and PYD domains-containing protein 3 (<i>NLRP3</i>)	0.8 *	1
	Pyrin (<i>MEFV</i>)	0.2 *	1
	Proto-oncogene c-Rel (<i>c-REL</i>)	0.6 *	1
	NF-kappa-B inhibitor alpha (<i>IκBα</i>)	1.2 *	0.9
	NF-kappa-B p100 subunit (<i>NF-κB2</i> or <i>P52</i>)	0.8 *	1.1

	Tumor necrosis factor receptor superfamily member 5 (<i>TNR5</i> or <i>CD40</i>)	0.7 *	1
	NACHT, LRR and PYD domains-containing protein 1b (<i>NLRP1b</i>)	0.9	5 *
	NACHT, LRR and PYD domains-containing protein 12 (<i>NLRP12</i>)	1.2	0.5 *
	NLR family CARD domain containing 3 (<i>NLRC3</i>)	0.8	0.5 *
Wnt/β-catenin signaling	Transcription factor 7-like 2 (<i>TCF7L2</i>)	0 *	2
	Adenomatous polyposis coli protein (<i>APC</i>)	0 *	10.2 *
Neurogenesis	Paired box protein Pax-6 (<i>PAX6</i>)	0.2 *	1.6 *
	LIM/homeobox protein Lhx2 (<i>LHX2</i>)	0.7 *	1.7 *
	GATA-binding factor 3 (<i>GATA3</i>)	0.6 *	0.9
	Pre-B-cell leukemia transcription factor 1 (<i>PBX1</i>)	1.4	4.1 *
	Homeobox protein OTX1 (<i>OTX1</i>)	0.7	1.4 *
	Transcription factor SOX-2 (<i>SOX2</i>)	0.9	1.3 *
	Transcription factor SP8 (<i>SP8</i>)	1	1.4 *
Axonogenesis	Serpin family E member 1 (<i>SERPINE1</i>)	14.5 *	1.4
	Secreted protein acidic and cysteine rich	1.5 *	1

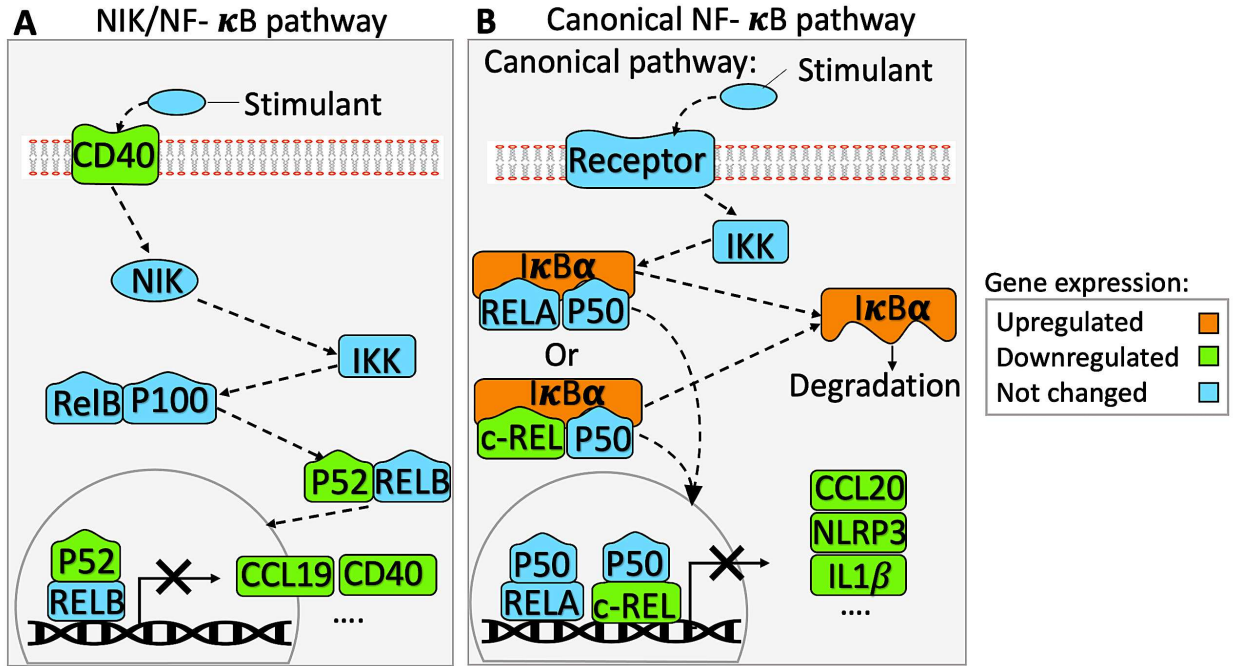
(SPARC)

A disintegrin and metalloproteinase with thrombospondin motifs 1 (<i>ADAMTS1</i>)	2.8 *	1
Fibroblast growth factor receptor 2 (<i>FGFR2</i>)	Inf *	0.7
Mesothelin-like protein (<i>MSLN</i>)	9.2 *	9.7 *
Fibronectin (<i>FN1</i>)	1.9 *	1.4
Neural-cadherin (<i>N-CAD</i> or <i>CDH2</i>)	0.6 *	0.8
Neural cell adhesion molecule 1 (<i>NCAM1</i>)	0.2 *	0.8
Netrin-1 (<i>NTN1</i>)	1.7 *	1.4
Ephrin type-A receptor 4 (<i>EPHA4</i>)	2.1 *	0.8
N-acetyllactosaminide beta-1,3-N- acetylglucosaminyltransferase (<i>β3GNT1</i>)	2.5 *	1.3
Transcription factor AP-1 (<i>JUN</i>)	0.2 *	0.7
Partitioning defective 3 homolog (<i>PAR3</i>)	0 *	2.7 *
Biogenesis of lysosome-related organelles complex 1 subunit 1 (<i>BLOC1S1</i>)	1.1	1.5 *
Epidermal growth factor receptor substrate 15 (<i>EPS15L1</i>)	0.9	Inf *

Phosphatidylinositol-binding clathrin assembly protein (<i>CALM</i>)	2.2	33.3 *
Ras-related protein Rab-3A (<i>RAB3</i>)	1	1.5 *
Ras-related protein Rab-10 (<i>RAB10</i>)	1	1.4 *
Roundabout Homolog 2 (<i>ROBO2</i>)	0.9	1.5 *
T-lymphoma invasion and metastasis- inducing protein 1 (<i>TIAMI</i>)	1.2	1.6 *
Microtubule-associated protein 1A (<i>MAP1A</i>)	1.2	1.7 *
Microtubule-associated protein 1B (<i>MAP1B</i>)	1	1.7 *
Tripartite motif-containing protein 46 (<i>TRIM46</i>)	1	2.1 *

806

807



808

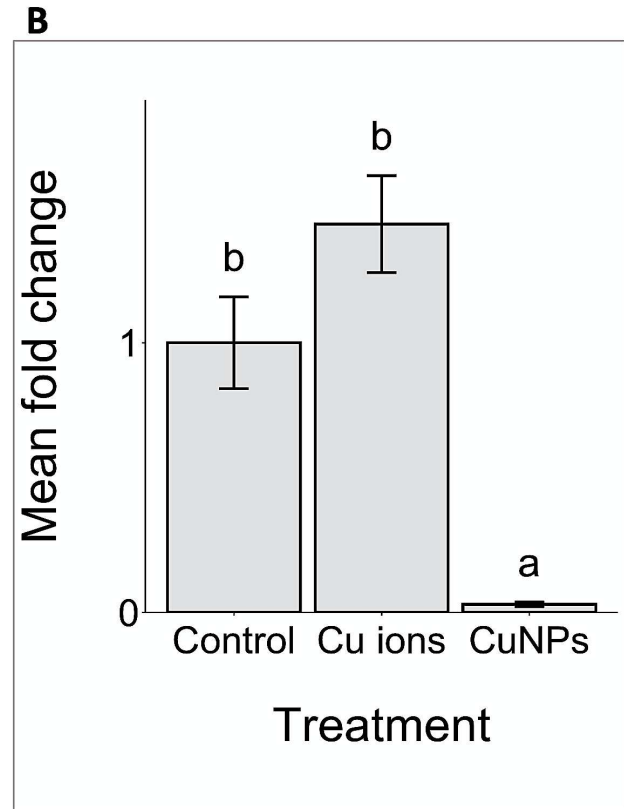
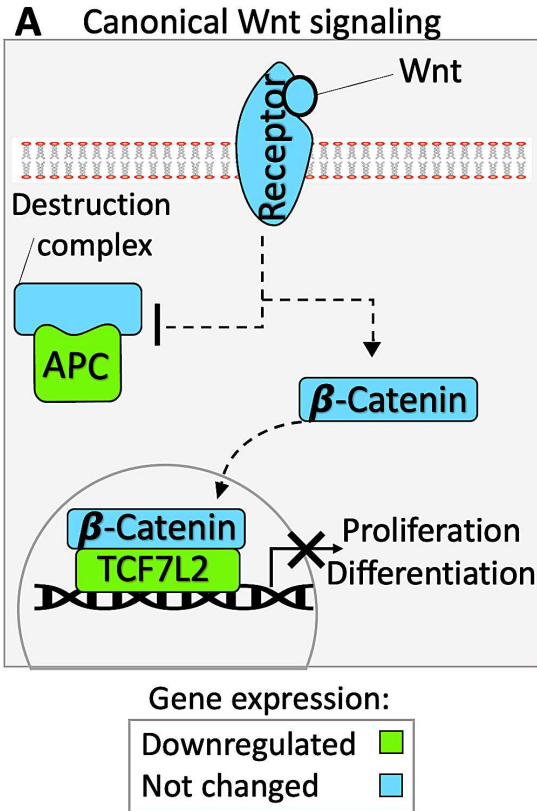
809 Figure 3. Schematic representations of transcriptional alterations in NF- κ B signaling pathways

810 following exposure to CuNPs in rainbow trout olfactory mucosa. (A) NIK/NF- κ B signaling

811 pathway. (B) canonical NF- κ B signaling pathway. The colour-coded legend represents the

812 transcription pattern of the differentially expressed genes.

813



814

815

816 Figure 4. Effect of CuNPs on the transcription of genes involved in canonical Wnt signaling
 817 pathway in the rainbow trout olfactory mucosa. (A) Schematic representation of canonical Wnt
 818 signaling pathway in the CuNP treatment. The colour-coded legend represents the transcription
 819 pattern of the differentially expressed genes. (B) The relative expression of *TCF7L2* in response
 820 to different Cu treatments in the olfactory mucosa. The gene expression was measured by qPCR.
 821 Lower-case letters indicate significant differences ($p \leq 0.05$, error bars ± 1 SEM).

822

823